



# Final Technical Report: "III-V Modulation and Switching Devices for Optical Systems Applications"

AFOSR-91-0434

Principal Investigator:  
Professor Jasprit Singh

Co-Principal Investigator:  
Professor Pallab Bhattacharya

Department of Electrical Engineering and Computer Science,  
The University of Michigan, Ann Arbor, MI 48109-2122

Air Force Office of Scientific Research  
Bolling Air Force Base

April, 1995

Accession For	
NTIS CRA&I	<input checked="checked" type="checkbox"/>
DTIC TAB	<input type="checkbox"/>
Unannounced	<input type="checkbox"/>
Justification .....	
By .....	
Distribution /	
Availability Codes	
Dist	Avail and/or Special
A-1	

## Multiple Quantum Well Based Devices for Systems Applications – Final Report – 4/10/1995

The thrust for this three year program has been to develop novel devices and systems applications for multiple quantum well based devices. We have investigated architectures based upon the quantum confined Stark effect (QCSE), a means by which excitonic resonances in a quantum well are electric field tuned to shift the peaked absorption spectrum of the material. This devices based upon this concept have been used, in the past, to realize switching structures employing the characteristic negative differential resistance available in PIN-MQW diodes under illumination. We have focuses, primarily on three schemes based upon the QCSE, to extend the utility of quantum well based devices. Firstly, we have developed, tested and optimized a novel tunable optical filter for wavelength selective applications. Secondly, we have demonstrated an MQW based scheme for optical pattern recognition which we have applied towards header recognition in a packet switching network environment. Thirdly, we have extended previous MQW based switching schemes to implement an optical read only memory (ROM) which can store two bits of information on a single sight, read by two different probe wavelengths of light.

### A Voltage Tunable Multiple Quantum Well Distributed Feedback Filter with an Electron Beam Written Schottky Grating

Distributed feedback structures utilizing carrier based tuning have been extensively investigated for communications applications by virtue of their extremely narrow transfer characteristics. Two difficulties, however, limit the performance and applicability of such devices, namely, a carrier lifetime limited tuning speed and the low yield of regrowth. A novel optoelectronic filter with voltage-tunable transfer characteristics has been developed and implemented in a GaAs/AlGaAs multi-quantum well(MQW) waveguide device to circumvent these two problems.

By virtue of the quantum-confined Stark effect (QCSE), the refractive index in quantum wells has a strong dependence on a transverse applied field across the wells. This dependence can be quantified using the Kramers-Kronig relation to the well known absorption shift due to the QCSE and is seen to be stronger than the bulk electro-optic effect in GaAs. The refractive index at the periphery of a guiding region can be given a periodicity in the guiding direction by application of a bias on an electron-beam patterned Schottky grating atop the

guide (Fig 1). If the period of the Schottky grating and associated index profile satisfies the Bragg condition, as in a resonant distributed feedback (DFB) structure, band-reject filtering results. Altering the bias on the Schottky grating changes the refractive index in the wells thereby changing the optical path length of the DFB structure and providing tunability of the wavelength at which Bragg diffraction occurs.

The device material structure, grown by MBE, is shown schematically in Fig 2 and resembles a typical wave guiding structure minus the thick upper cladding (which is formed by a subsequent PECVD oxide deposition). Transmission measurements were carried out on the waveguide device using a temperature tunable diode laser. For application of a 2V reverse bias on the grating, a shift in the resonance peak of  $8\text{\AA}$  occurs along with systematic peak broadening (Fig 3). For biases beyond 2V, absorption begins to dominate and filtering action is eclipsed.

Most recent work has consisted of increasing the number of grating lines in the device, which has produced a deeper filtering function (Fig 4), and performing numerical simulation of the fields in the structure, which has lead to an optimized filter structure. The optimized structure, incorporating a more efficient, nearly symmetric grating with a quarter wave shift, is expected to function as a band pass filter. Using coupled quantum wells, a greater tuning range owing to an expectedly higher electro optic coefficient will be achieved. For the realization of this optimized device, the electron beam grating definition parameters were altered to include proximity corrections (Fig 5) to correctly expose the grating fingers and connecting pads.

## Optical Header Recognition for Lightwave Switching Networks

The ability to route optical data in a switching network without optical to electronic to optical data conversion is highly desirable for high speed switching stations. We have developed an architecture for optical address header recognition based on a single multiple quantum well p-i-n (PIN MQW) modulator. For a digital optical pattern (a header), consisting of a true and complement pair, passing through a modulator whose time varying digital transmittance is phase-matched and complementary to the transitions of the incoming data, the output light, integrated over the word length will be a minimum. This minimum can then be discerned by a thresholding scheme to trigger optical data routing switches.

Such header recognition has been realized using a diode laser as a light source and a PIN MQW modulator to encode the data at the transmitting end. At the receiving node, another PIN MQW (Fig 6) is used as the 'Address' modulator. This architecture was tested at slow data rates for the purpose of a first demonstration. Recent thrusts have involved improving the systems aspects of the implementation to demonstrate a more applicable and

state-of-the-art capability. First of all, better modulation depth was realized, with the modulators now needing a 2.5V swing as opposed to 8V to achieve 24% modulation. Secondly, a higher speed demonstration was sought after. To this end, an HP80000 Programmable Data Generator System has been utilized to modulate the light in both the transmitting and receiving nodes. Using this equipment, modulation speeds of 1Gbps have been achieved and header recognition has been carried out at that speed. The best match of several test headers to a stored word was seen to produce a verifiable signature consisting of a minimum integrated output intensity over the length of the header (Fig 7). The HP80000 will allow the simulation of realistic ATM and Ethernet style data packets for the purpose of a demonstration of actual packet switching, which is the goal of this project.

The final aspect of this project has been to employ ECL based thresholding circuitry along with the proper timing circuitry in order to fully implement a switching network. A systems analysis was carried out to prove the feasibility of such a scheme with practical modulators and the circuitry is, at present, completed and fully functional and Mach-Zehnder based directional coupler switches based on the electro optic effect in quantum wells are in fabrication for the full demonstration of packet switching at a node.

### Dual Wavelength ROM for 2 bit storage on a single cell

There has been a recent push for the development of blue lasers for the goal of increasing storage density on optical read only memories (ROMs). By reducing the wavelength of the reading light by a factor of 2, increases in storage density of about 4 are obtained. Another way which we have been investigating to increase storage density of an optical ROM has been to store two bits of information on a single cell, read by two different wavelengths of light. We have developed and demonstrated the feasibility of this concept via the quantum confined Stark effect associated with placing a bias across quantum wells.

Examining the Stark shifted excitonic absorption spectra as shown in Fig 8a, we see that by carefully choosing two operating wavelengths, we can obtain transmittance (of the light through a quantum well region) versus field characteristics like that shown in Fig 8b. These characteristics are those of a two bit binary transfer function for the field magnitudes E1-E4. Our ROM device will be written by placing one of four of these field values across the quantum wells, and read by the transmittance of the two wavelengths of light through the wells.

The structure used to store the data is shown in Fig 9. As can be seen, by etching the top lightly doped layer to one of four calculated depths, the magnitude of the surface field which drops across the wells can be "Programmed". Experimental data shown in Fig 10 verifies the transmitted light has the predicted properties. To be a practically functioning scheme,

the contrast ratios for the on/off states of transmittance will need to be improved. These improvements will come as the growth techniques for quantum wells continues to mature.

### Summary

In summary, this ongoing project has served, over the years to bring to maturity the fabrication of advanced quantum well based devices, through the careful study of their physics. The most recent three years has extended this work to encompass novel device structures as well as larger scale systems implementations.

## Figure Captions

Figure 1 Waveguide shown schematically.

Figure 2 Wave guiding material structure as grown by MBE.

Figure 3 Transmission spectra of filter for 0, -1, -2 volts applied, showing DFB filtering resonances both broadening and shifting to longer wavelengths with increased bias.

Figure 4 A single shoulder of the filter function is shown for a device with increased grating periods. A deeper function has been realized.

Figure 5 A comparison of a contacted gratings written with identical electron beam doses a) Grating shown airbridged over a waveguide, with no proximity correction: several fingers not contacted. b) Contacted grating with proximity correction: all fingers perfectly contacted.

Figure 6 a) Schematic of modulator structure as used to store an address in a receiving station, shown for optical test input signal (011100) and modulator address (101010). b) Full system shown incorporating two such PIN MQWs

Figure 7 At a 1Gbps data rate, the modulated output at the receiving station is shown for four test patterns of varying degrees of error. For a stored word of (10100101), test patterns of (10100101), (10010110), (11010010) and (01011010) have 4,2,1,and 0 errors respectively. The time integrated powers show a minimum for the best match (0 errors). Integral taken as area under the curve for an arbitrary zero.

Figure 8 The quantum confined Stark effect shown for a) Two particular applied fields and b) Two particular wavelengths of light.

Figure 9 ROM structure grown by MBE and measured optically in transmission, showing etched steps.

Figure 10 Transmission of light through the four etched steps of the fabricated ROM shown for a) four applied magnitudes of field, and b) for the two correct values of wavelength from which arise two bit storage.

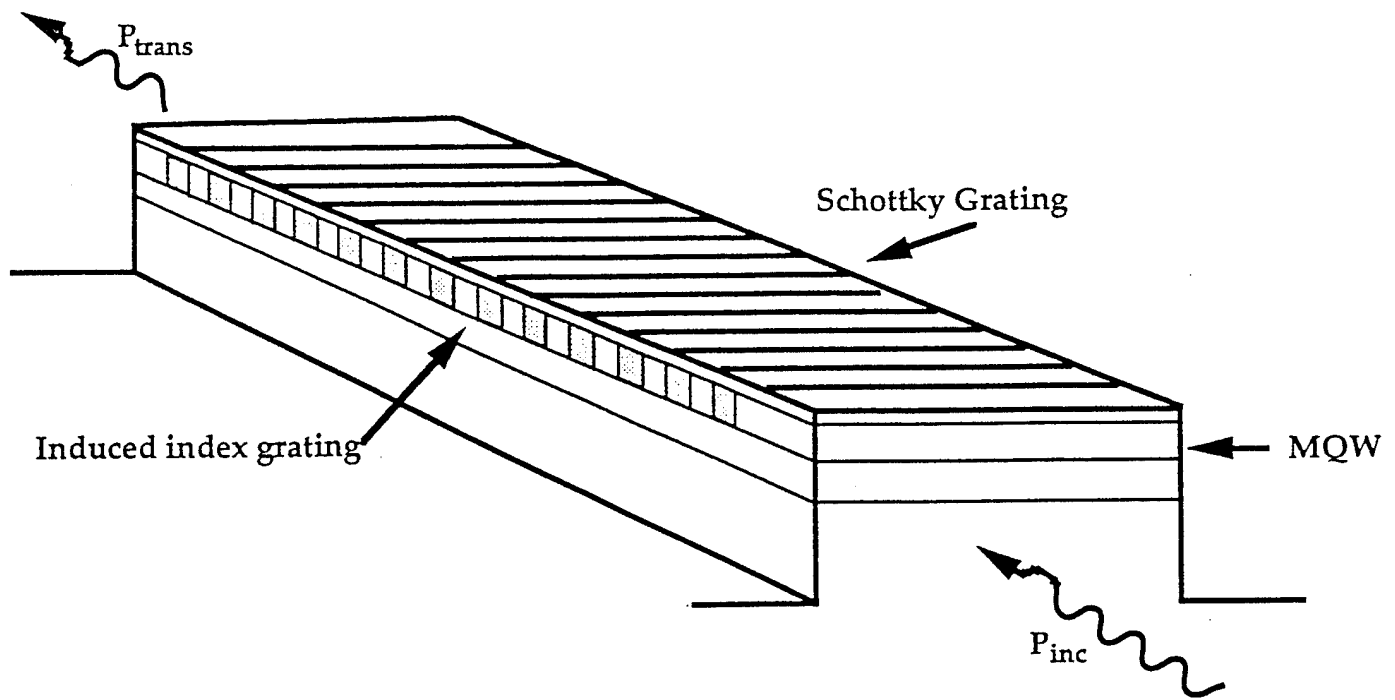


Fig. 1



200 Å	Al <sub>0.3</sub> Ga <sub>0.7</sub> As	n = 1.0 × 10 <sup>16</sup> cm <sup>-3</sup>
3 prd	GaAs/Al <sub>0.3</sub> Ga <sub>0.7</sub> As	
	L <sub>W</sub> = L <sub>B</sub> = 90 Å	undoped
0.3 μm	Al <sub>0.1</sub> Ga <sub>0.9</sub> As	undoped
0.5 μm	Al <sub>0.3</sub> Ga <sub>0.7</sub> As	n = 5.0 × 10 <sup>18</sup> cm <sup>-3</sup>
n+ GaAs Substrate		

Fig. 2

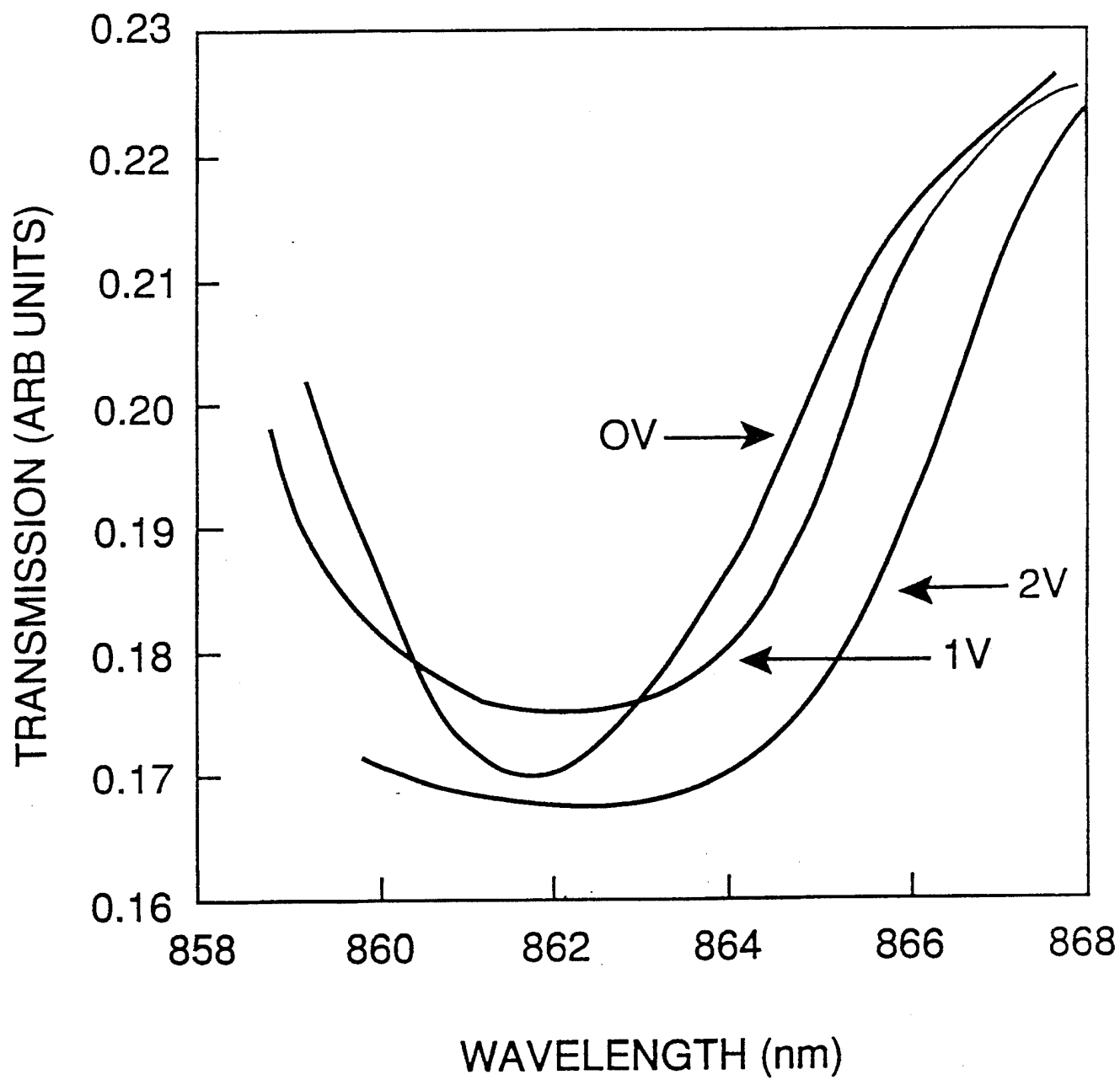


Fig. 3

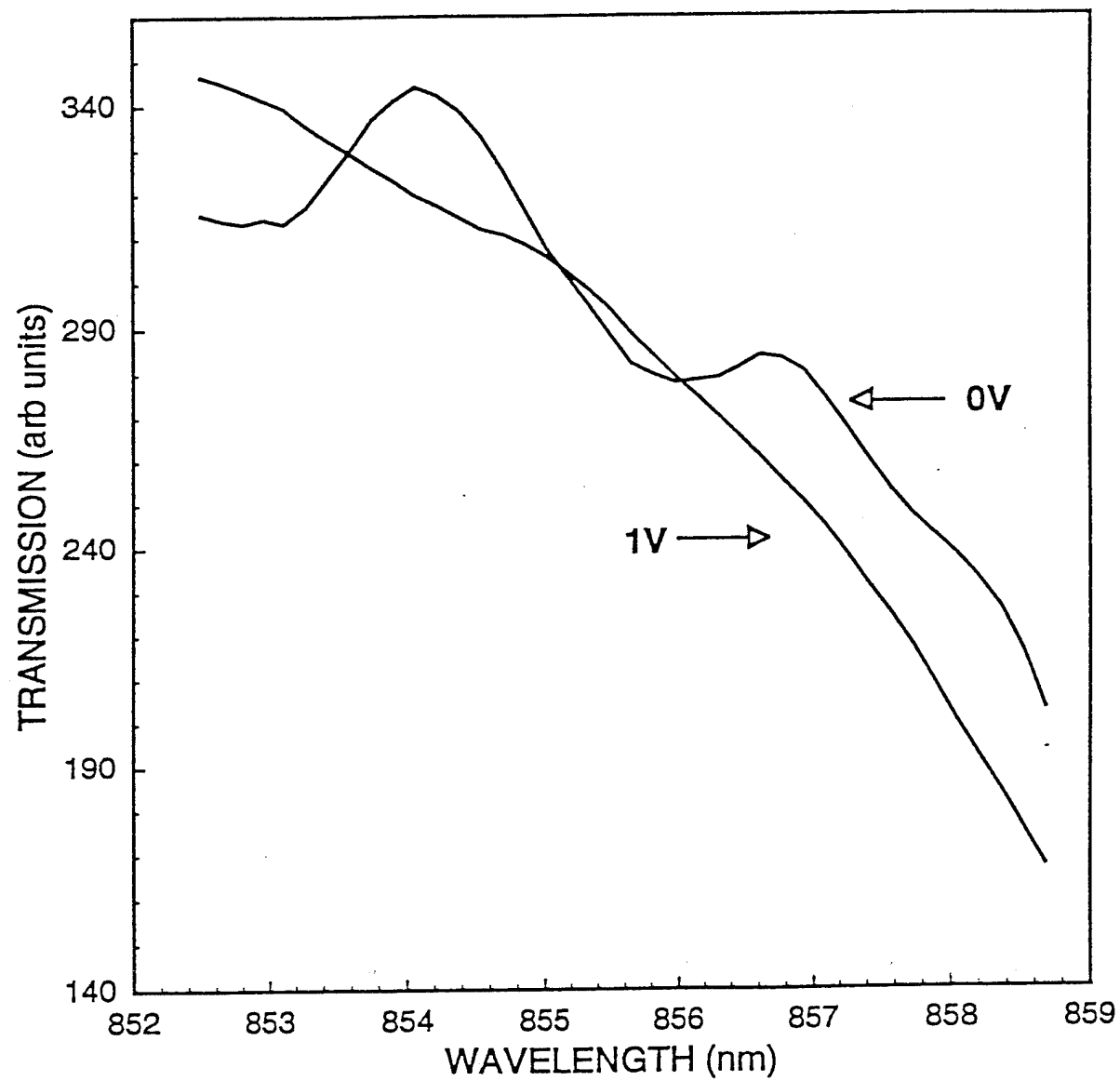
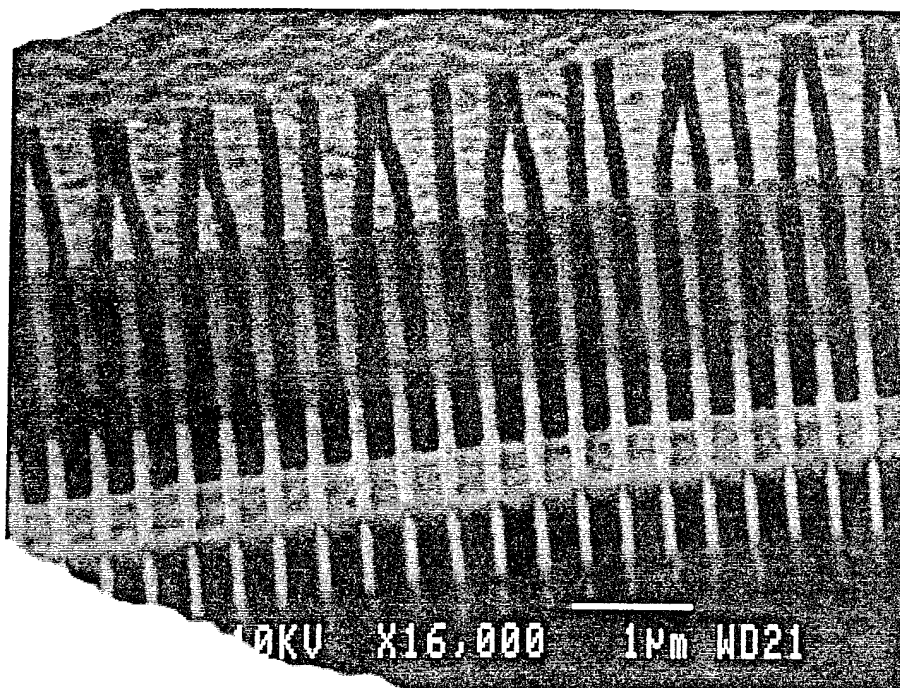
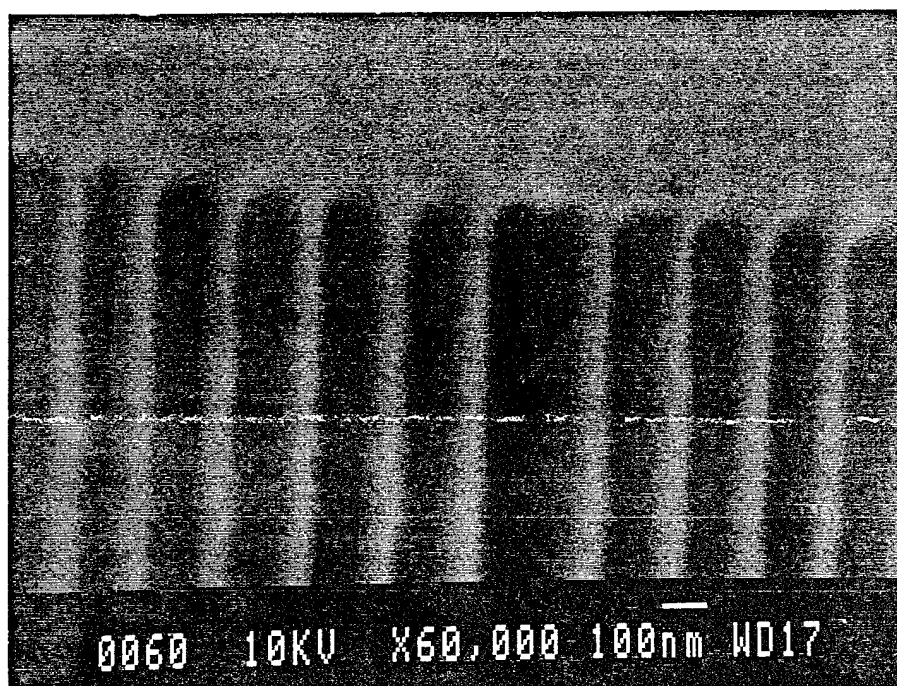


Fig. 4



(a)



(b)

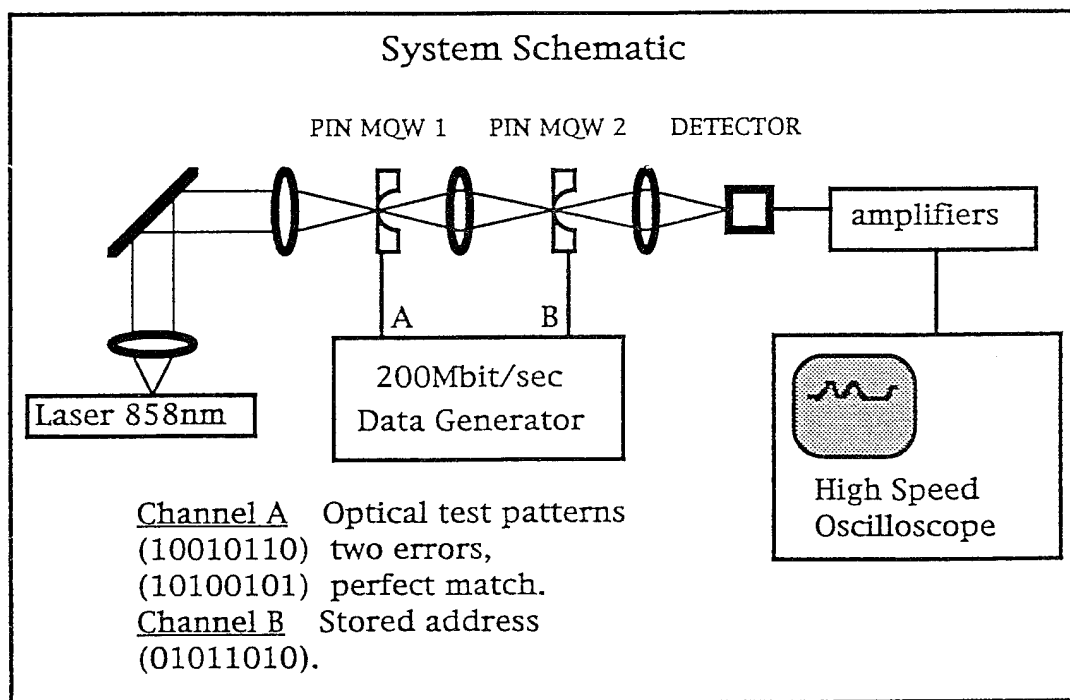
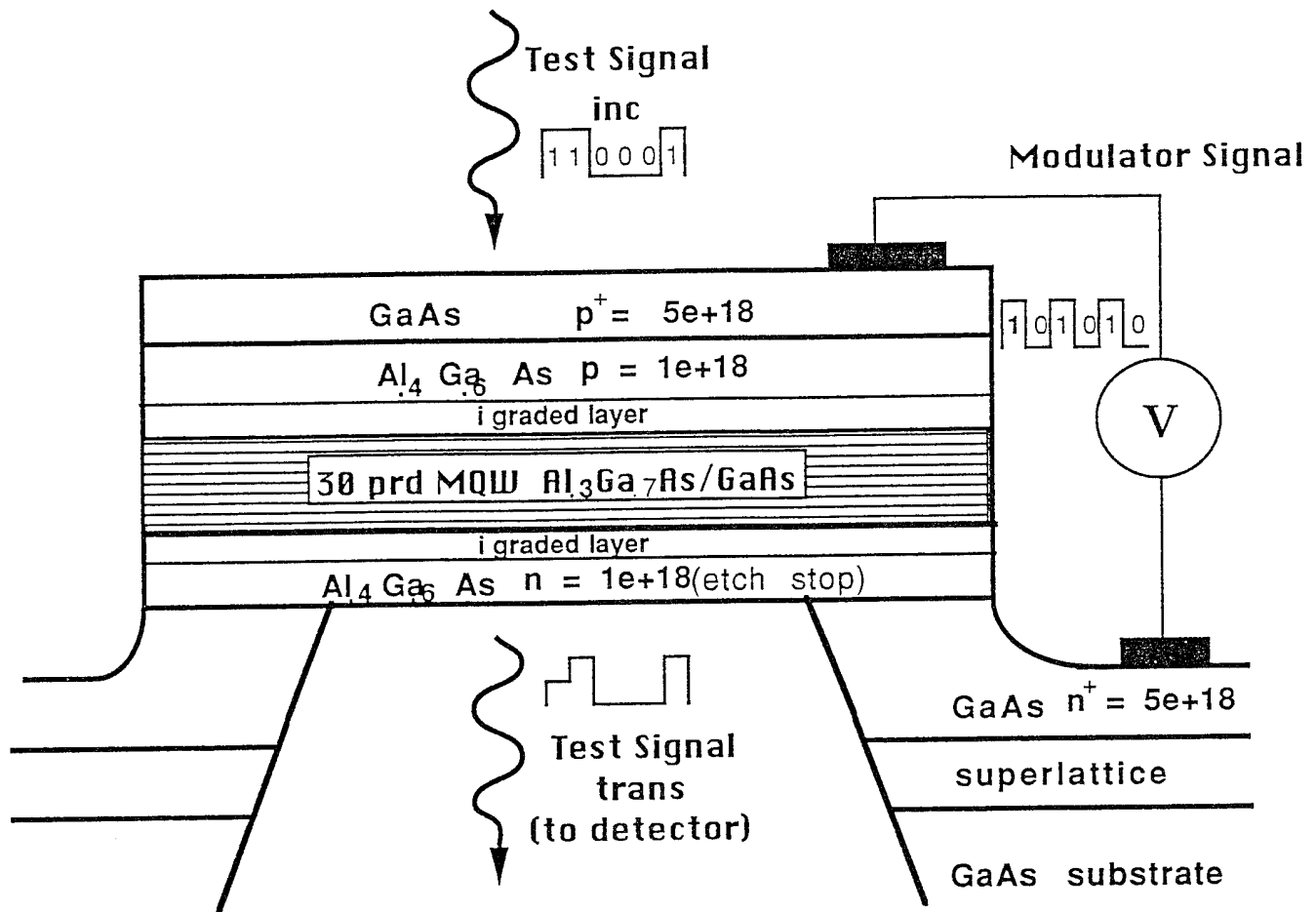
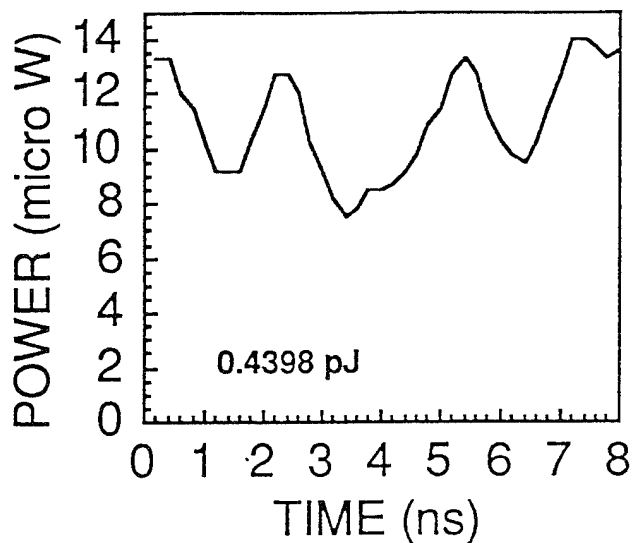
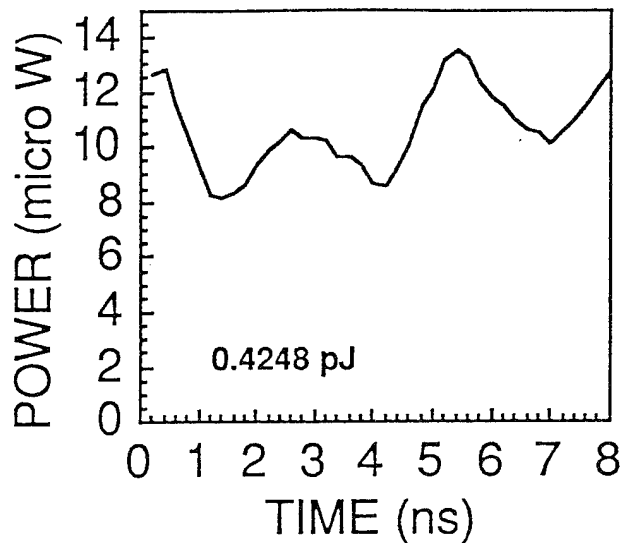


Fig. 6

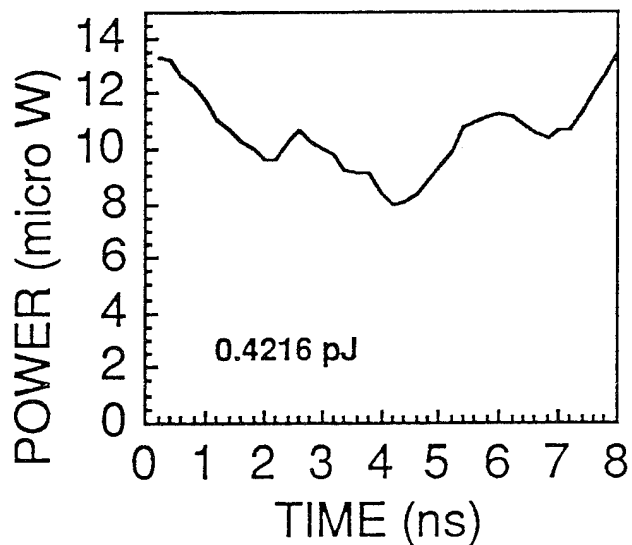
10100101 (4 mismatches)



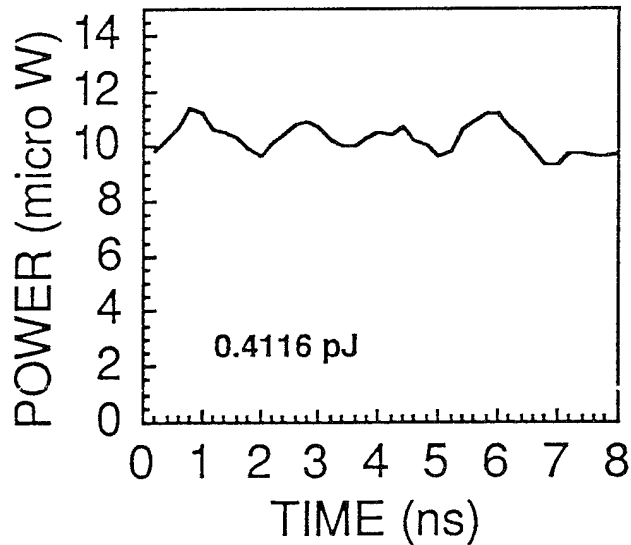
10010110 (2 mismatches)



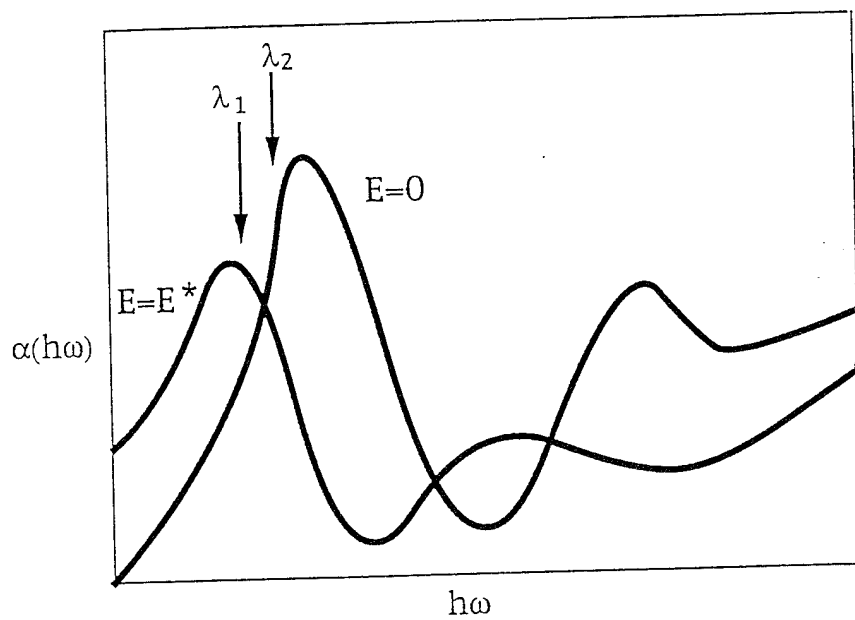
11010010 (1 mismatch)



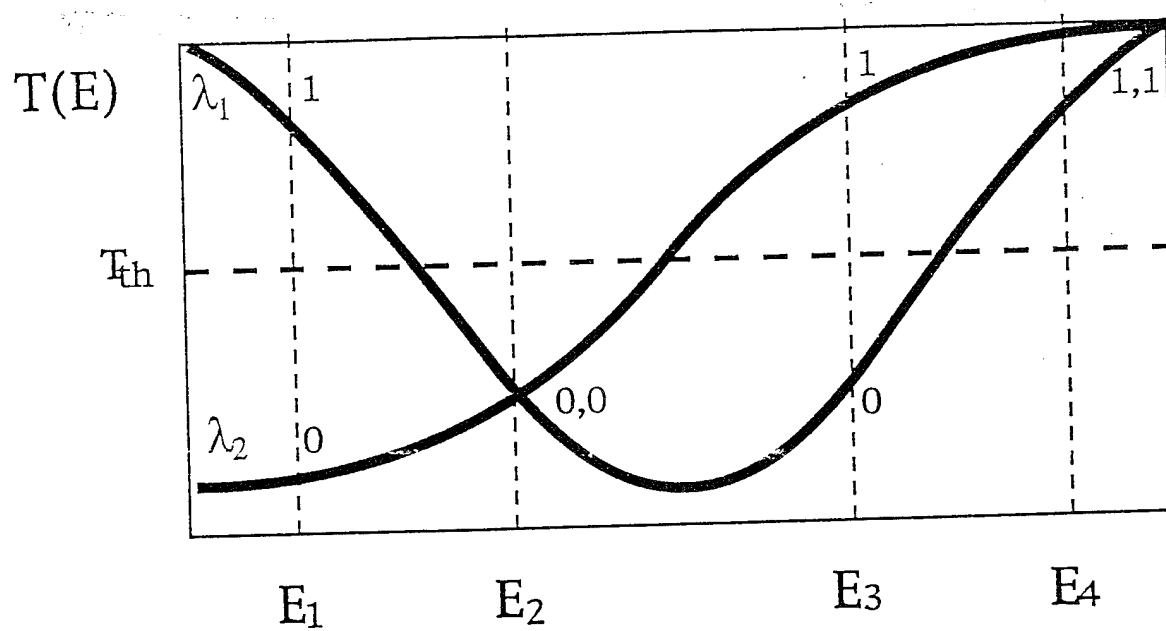
01011010 (correct)



Energy per word (area under curve) is a minimum for best match



(a)



(b)

Fig. 8

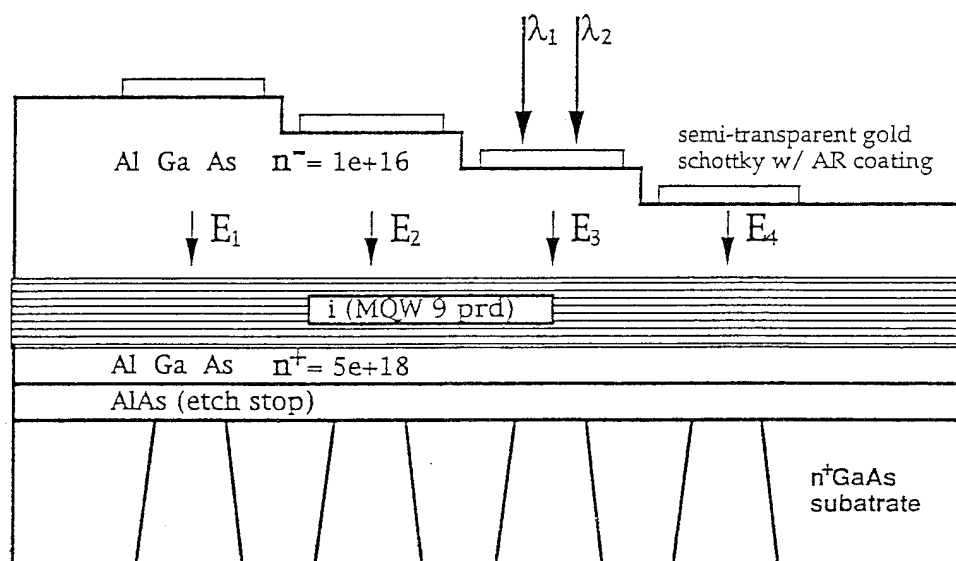
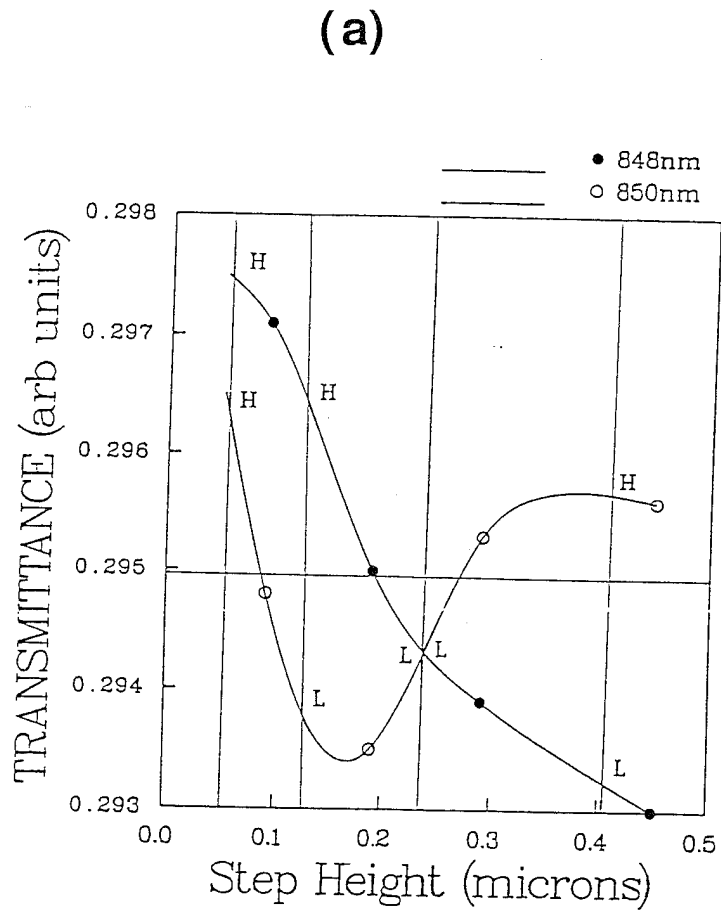
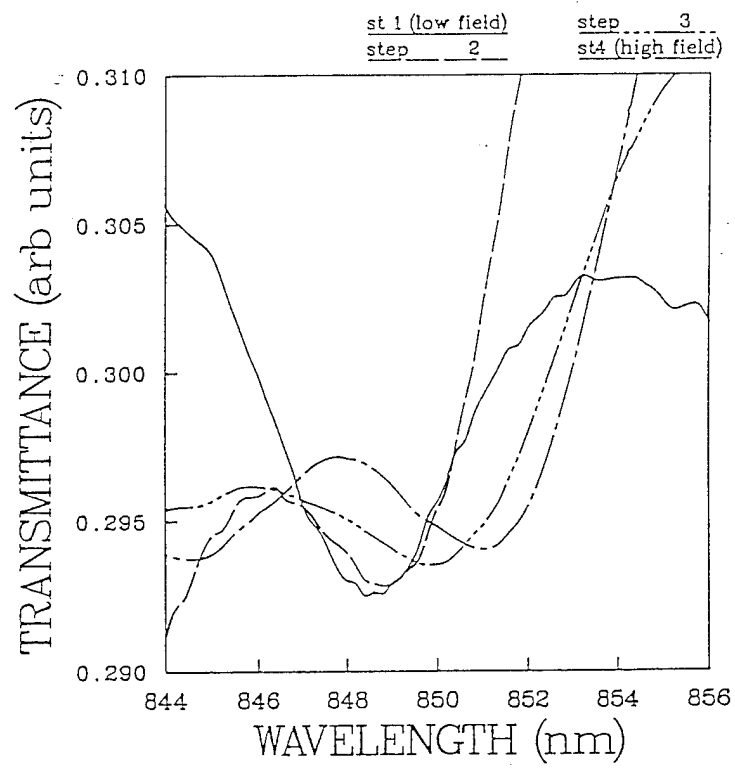


Fig. 9





(b)

Fig. 10